Adaptive delays alignment in polar transmitter architecture

J.-F. Bercher[1] and C. Berland[2]

[1] Université Paris-Est, LabInfo-IGM, ESIEE-Paris
[2] Université Paris-Est, Département Systèmes électroniques, ESIEE Paris
Cité Descartes, BP99, 93162 Noisy le Grand cedex
{jf.bercher,c.berland}@esiee.fr

***Abstract*—Polar architecture is a regarded solution for the design of efficient transmitters for radiocommunication systems. However, this architecture is sensitive to delay mismatches between the envelope and the phase paths. In this paper, we propose to address this problem by baseband digital signal processing. We present several adaptive algorithms based on the minimization of the mean square error between the ideal signal and the signal generated by the transmitter. Since the system gain and phase offset of the system are not precisely known, we also consider the problem of the identification of these quantities in the feedback loop. We propose solutions for the direct correction of the unknown delays, which also account for the gain variation and phase offset. A model of a polar architecture is tuned on Agilent Advanced Design System and used to evaluate the algorithms. Results assess both the need of a calibration procedure and the relevance of the proposed solutions. We draw attention to the improvement of the transmitter performances using these algorithms and point out the potential of digital signal processing in transmitter design.**

***Index Terms*—Polar transmitters, EER architecture, time alignment, delays, calibration, baseband signal processing, least mean square methods**

I. Introduction

Since new applications and upcoming standards require increasing data rates and lower power consumption, the study and development of new architectures of communication transmitters for user units is very active. In particular, architectures relying on the polar representation of signals, called polar transmitters, are highly regarded. Indeed, the polar architecture is a solution to achieve a very efficient and linear transmitter [1]. Further, it is flexible enough to enable the development of multiband [2] and multimode solutions [3], [4] for Software-Defined Radio (SDR). This architecture is based on Kahn's Envelope Elimination and Restoration (EER) procedure [5]. It has been improved so that actual solution tends toward a quasi fully digital transmitter [6]. The phase-modulated signal is translated to RF frequency using either a classical I/Q modulator or through a modulated phase locked loop. The envelope is restored at the output of the transmitter by varying the supply of the power amplifier (PA) through a switching power supply.

The drawback of this architecture is its sensitivity to the difference of propagation and processing delays between amplitude and phase signals paths. The mismatch between the two paths entails spectral regrowths [7], [8] and an increase of the Error Vector Magnitude (EVM) [9]. Fulfillment of the strict requirements on transceivers for modern modulation schemes warrants a high precision timing alignment between the envelope and phase path [10]. This becomes more and more critical and challenging as the data rate increases [10], [11], [12].

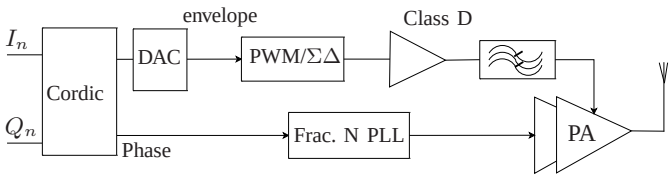

Fig. 1. Polar transmitter. Instead of the classical I-Q decomposition, the polar transmitter rely on the polar decomposition of signals. Here a CORDIC processor (Coordinate Rotation Digital Computer) is used. The phase-modulated signal is translated to RF frequency using a modulated phase locked loop, either digital or analog. The envelope is restored at the output of the transmitter while varying the supply of the power amplifier (PA) through a switching power supply. A drawback of the architecture is its sensitivity to the differential processing delay between the two paths.

This mismatch is due to pipeline differences in the paths and to the delay in the anti-alias filter (amplitude path), as well as small contributions from other analog delays [13]. The asymmetry of processing, the independence of underlying clocks and the analog interfaces also imply delay mismatches in the recent fully digital solutions, which also require a precise delay alignment of amplitude and phase paths [14]. In a production environment, even with the global knowledge of various delays in the transmitter path, these delays have to be tuned on a case-by-case basis to include process spreading on elements. Overall, this mismatch becomes more and more limiting as data rate increases. Furthermore, current devices experience severe variations of temperature, modifications of the supply voltage, output frequency and power [15] that impact the system behavior and can also imply further time-varying desynchronizations that, according to their amount, would need a tracking procedure.

A linear interpolation was suggested in [16] so as to compensate for the mismatch, while a group delay equalizer was proposed in [17]. In these two cases, it still remains to identify the delay mismatch and track its possible variations. An adaptive hardware realization was proposed in [18], but with a precision limited by the underlying clock. A calibration

procedure, based on a feedback loop and the maximization of the input-output covariance function, is described in [19].
We elaborate here on the principle of an adaptive delay correction presented in [20], [21]. We propose solutions that cover the correction and tracking of the unknown delays, with high accuracy and low complexity. We also show that the solutions are robust to further mismatches, such as uncertainty in the knowledge of gain and phase shift of the transmitter. We still propose a solution for the identification of this complex gain in order to lower the residual noise and improve the performances. The effectiveness of the solution is illustrated on the case of the 3GPP standard for UE transmitters.
The paper is organized as follows. In section II, we present the model of the architecture considered, we illustrate the need of envelope and phase alignment, and discuss its feasibility in polar based transmitter architectures. We also analyze the main characteristics of the mean square error between the input and output of the system. In section III, we consider the problem of the delays correction, based on the minimization of the input-output means square error. We propose and argue a correction algorithm, implemented using a stochastic gradient. In order to reduce its complexity, we also describe a suboptimal version of this correction algorithm. The performances of these two solutions are assessed by simulations. In section IV, we consider the behavior of these solutions subject to uncertainties in the knowledge of system gain and phase offset. In order to preserve good performances, we introduce an identification of these unknowns in the feedback loop. The efficiency of the whole solution, in terms of convergence speed, error vector magnitude and spectral regrowths, is then demonstrated through simulation results. We finally conclude in section V.

II. Envelope and phase alignment

In this section, we first indicate that envelope and phase alignment is an essential issue in the design of polar transmitters for modern systems. We discuss the feasibility of the alignment of the envelope and phase components.Then, we examine the behavior of the mean square error between the original signal and the signal at the output of the transmitter, and consider the minimization of this mean square error as a possible basis for the compensation of the delay mismatches.

A. Simulation model of the transmitter – Impact of delay mismatches on a 16QAM modulation

In this paper, we will illustrate the issues and the performances of proposed algorithms on a 16QAM modulation with a data rate of 3.84 Mcps. This corresponds to the 3GPP standard [22]. Transmitter characteristics are given in term of EVM (Error Vector Magnitude), spectrum transmitter mask and ACLR. We will mainly focused the performances observations on EVM and output spectrum. The output spectrum is specified relative to the root-raised cosine filtered mean power of the UE carrier taken at different frequency offsets from the carrier. Specifications are as follows:

- at 2.5 MHz, -35 dBc in 30 kHz bandwidth,
- at 3.5 MHz, -50 dBc in 30 kHz bandwidth,
- at 4 MHz, -35.5 dBc in 1 MHz bandwidth,
- for F>8 MHz, -49 dBc in 1 MHz bandwidth.

The EVM has to remain lower than 17.5%.
The transmitter model, see Fig. 2, is elaborated with Agilent Advanced Design System (ADS). The complex modulated signal is generated with a 16QAM modulator, followed by a 0.22 roll-off root-raised cosine filter. A complex to polar conversion is then realized, with a quantization on 10 bits at a sample frequency of $T_s/12$. Conversions to the analog domain are realized using oversampling DACs followed by baseband filters. The processing delays, as well as delays introduced by filters and other analog elements, are modeled as two delays Δ_1 and Δ_2 in the envelope and phase paths respectively. As we will describe in the following sections, the correction algorithms involve the comparison between the ideal signal and the transmitted one. Hence, a return path has to be implemented, using either an I/Q demodulator or a simple frequency translation (depending on the algorithm) and an analog to digital conversion. The signal is quantified on 10 bits and the converter uses the same clock as in the transmit path, that is to say with a sampling rate of $T_s/12$. Finally, we introduce a complex gain to account for the gain and phase rotation of the modulated signal after the power amplifier. In this work we do not elaborate further on the model of the power amplifier and only take into account a gain and phase rotation. Potential nonlinear effects, especially, are not considered here where we concentrate on the issues related to time mismatches. The calibration and correction of nonlinearities, which usually involves a feedback loop, is well documented, but still an open issue [23].
With this model, without gain, phase rotation or time mismatches, the output EVM is on the order of 0.3%, due to the quantification on 10 bits. Spectral regrowth at $3.5MHz$ from the carrier is at $-70dBc$.
In order to examine the sensitivity of polar architecture to delay mismatches between phase and envelope paths, we introduced into the simulation model delay mismatches from $T_s/2$ to $T_s/50$. Impacts of these mismatches on the EVM value and the output spectrum are presented Table I.

Delay	**EVM (%)**	**Relative Spectrum @**$3.5\ MHz$
$T_s/2$	77%	-33 dBc
$T_s/10$	12.4%	-48 dBc
$T_s/20$	6.5%	-55 dBc
$T_s/50$	3.6%	-61 dBc

TABLE I
Impacts of delay mismatches on the EVM and on the spectrum.

According to specifications such as 3G specification concerning the EVM and spectrum specifications, a maximum acceptable delay shall be on the order of $T_s/50$, with $T_s = 0.26\ \mu s$ the symbol period, that is to say lower than 5 ns. These results demonstrate that a synchronization algorithm is mandatory.

B. Feasibility of the time alignment

Let

$$X(t) = \rho(t)\exp(j\phi(t)) = \rho(t)\cos(\phi(t)) + j\rho(t)\sin(\phi(t))$$

be the complex envelope of the signal at the output of the digital modulator, where $\rho(t)$ and $\phi(t)$ are the envelope and

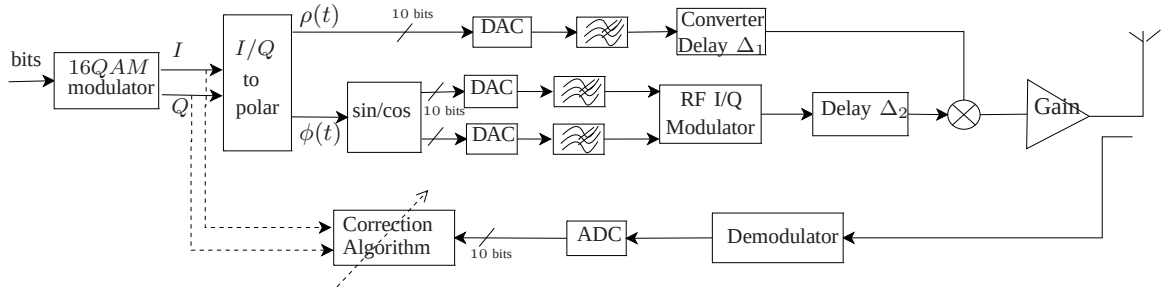

Fig. 2. Simulation model of the transmitter. This model includes an I/Q modulator followed by an I/Q to polar converter. The envelope signal is converted into analog using a 10 bits DAC. In the envelope path, the impact of the DC-DC converter is modeled as a delay Δ_1. The phase signal is translated to RF with an RF I/Q modulator after being converted with 10 bits DACs. The processing delay is introduced as a delay Δ_2 before the restoration of the complete modulated signal. A complex gain in the return path accounts for gain and phase shifts that affect the emitted signal.

phase signals, as shown in the model Fig. 2.

The baseband signal $X(t)$ is processed by the RF transmitter (shaping, RF translation, amplification) which results in the signal at the antenna, whose baseband complex envelope is denoted $Z(t)$. This signal is affected by the delays introduced by the RF processing. The envelope and phase components are delayed respectively by Δ_1 and Δ_2. The signal $Z(t)$ then becomes

$$Z(t) = \rho(t-\Delta_1)\exp\left(j\phi(t-\Delta_2)\right).$$

For complex modulation schemes, $X(t)$ can often be modelled as a complex Gaussian process. In the case of a complex circular Gaussian process it is well known that envelope $\rho(t)$ and phase $\phi(t)$ are independent and respectively distributed according to Rayleigh and uniform distributions.

The case of delayed envelope and phase is less known. In fact, it appears that $\rho(t-\Delta_1)$ and $\phi(t-\Delta_2)$ are also Rayleigh and uniform independent variables, with no reference to the correlation structure of the underlying original Gaussian signal $X(t)$, for any delays Δ_1, Δ_2, see [9]. This result indicates that for Gaussian processes, envelope and phase are *always* independent whatever the delay between envelope and phase components. This shows that the statistics of the output at a single instant do not convey any information on the time alignment or mismatch between envelope and phase components. Hence, any solution must involve statistical quantities computed from several instants. A simple example is the correlation function, or equivalently the power spectrum. If $z(t) = \mathrm{Re}\{Z(t)\}$, denotes the real part of the output, its correlation function is

$$\begin{aligned} R_{zz}(\tau) = \mathrm{E}\{&\rho(t-\Delta_1)\cos(\phi(t-\Delta_2)) \\ &\times\rho(t-\tau-\Delta_1)\cos(\phi(t-\tau-\Delta_2))\} \end{aligned} \quad (1)$$

where $\mathrm{E}[\bullet]$ denotes the statistical expectation operator. The point that we must emphasize here is that we do not have a closed-form expression for $R_{zz}(\tau)$, unfortunately, and it even does not seem possible to obtain a workable series representation. Series expansion exist for the correlation of the $\cos(\phi)$ term, or for the correlation of the envelope [24]. Consequently it is difficult to quantify the dependence of the correlation function on the delay mismatch and imagine a procedure relying only on this correlation function. However, introducing a delay μ in the envelope path (for instance), denoting $\Delta = \Delta_2 - \Delta_1$ and using the stationarity of the signal, we obtain

$$\begin{aligned} R_{zz}(\tau,\mu) = \mathrm{E}\{&\rho(t-\mu)\cos(\phi(t-\Delta)) \\ &\times\rho(t-\mu-\tau)\cos(\phi(t-\Delta-\tau))\}. \end{aligned} \quad (2)$$

Then we can observe that this new correlation function is exactly equal to the correlation function of the original aligned signal $R_{xx}(\tau)$ when $\mu = \Delta$. Therefore, a possible procedure can be to look (numerically) for μ that minimizes some distance between $R_{zz}(\tau,\mu)$ and $R_{xx}(\tau)$, for any τ, e.g.

$$\int \left(R_{zz}(\tau,\mu) - R_{xx}(\tau)\right)^2 \mathrm{d}\tau, \quad (3)$$

or equivalently in the frequency domain:

$$\int \left(S_{zz}(f,\mu) - S_{xx}(\tau)\right)^2 \mathrm{d}f. \quad (4)$$

From these two procedures, we can yet observe that (i) we need a feedback from the output, that is a way of acquiring and computing some quantity related to the output of the system, and (ii) we need to compare it to some known or estimated characteristic of the input signal. This means that we shall implement a feedback loop, relying on the demodulation and digitization of an image of the emitted signal taken with a coupler. It shall be observed that a feedback loop is often already present for calibration or tracking purposes (namely for the power amplifier calibration and control).

But the two suggestions above are actually difficult to implement because they require the evaluation of (integrals or sums of) correlation functions, or spectra, which is computationally expensive and statistically delicate; the control algorithm can not be derived precisely, nor characterized, because of the lack of closed form expression of the correlation. Let us finally observe that it is, in principle, possible to evaluate only some portion of the output spectrum and tune the relative delay so as to minimize the spectral regrowths. The drawback of such a solution is the definition of the minimization procedure, the existence of local minima, the fact that outband levels can be extremely low with high variance.

Since we see that a feedback loop is almost unavoidable, our proposal is to consider the direct error between the input and output signals and examine the possibility to derive compensation procedures of the delay mismatches based on this error.

C. The mean square error between the original and generated signals

As above-mentioned, we note $X(t)$ the complex envelope of the signal at the output of the digital modulator and $Z(t)$ the baseband complex envelope of the signal at the antenna. Let us define by

$$J(\Delta_1, \Delta_2) = \mathrm{E}\left[|e(t)|^2\right] = \mathrm{E}\left[|x(t) - z(t)|^2\right] \tag{5}$$

the mean square error between these two signals, with $x(t) = Re\{X(t)\}$ and $z(t) = Re\{Z(t)\}$.
Taking into account the independence between $\rho(t_1)$ and $\phi(t_2)$, for any instants t_1, t_2, it reduces to

$$J(\Delta_1, \Delta_2) = 4R(0,0) - 4R(\Delta_1, \Delta_2) \tag{6}$$

where

$$R(\Delta_1, \Delta_2) = \mathrm{E}\left[\rho(t)\cos(\phi(t))\rho(t-\Delta_1)\cos(\phi(t-\Delta_2))\right] \tag{7}$$

is a kind of 'correlation function'. As already indicated, we do not have a closed form expression for $R(\Delta_1, \Delta_2)$. Therefore, we must rely on numerical simulations or approximations to quantify the behavior of the algorithms presented in the following sections.
We can still note here that $R(0,0)$ reduces to $R(0,0) = \mathrm{E}\left[\rho(t)^2\right]\mathrm{E}\left[\cos(\phi(t))^2\right]$, and that $R(\tau,\tau)$ obtained with $\tau = \Delta_1 = \Delta_2$ is nothing else but the correlation function $R_{xx}(\tau)$. Since we know that the correlation function is a function of the shaping filter, it follows that the behavior of the error $J(\Delta_1, \Delta_2)$ is closely related to the shaping filter. We shall also note that $J(\Delta_1, \Delta_2) = \int S_{ee}(f)\mathrm{d}f$, where $S_{ee}(f)$ is the power spectrum of the error $e(t)$. Hence, the mean square error $J(\Delta_1, \Delta_2)$ also represents the power spectrum of the error induced by the mismatches Δ_1 and Δ_2, including the spectral regrowths.
The error function $J(\Delta_1, \Delta_2)$ was evaluated numerically in the case of a 16QAM modulation with a square-root Nyquist filter (root-raised cosine with 0.22 roll-off) and a sampling rate of 16 samples per symbol. It is presented in Fig. 3 for delays lower than 3 symbol periods. We clearly observe a global minimum, but some local minima also appear for more important delays. Therefore, one can define a basin of attraction $\mathcal{C}$, as reported in Figs. 3 and 4 such that any descent algorithm will converge efficiently to the global minimum. This indicates that it is possible to adjust efficiently some parameters on the input or the output in order to minimize the resulting error. With such an approach, we might be able to account for delays that belong to the domain of convergence in Fig. 4. If this domain of convergence is too restrictive, it is still possible to enlarge it by designing specific training sequences with a smoother error function (but this supposes a pre-calibration approach).
Because of the degradation of performances as discussed before, it is mandatory to counterbalance the relative delay $\Delta_2 - \Delta_1$ between the two components at the antenna. A natural approach is to identify these delays, see [20], and then correct them. But it is also possible to directly compensate the delays without requiring a preliminary identification step.

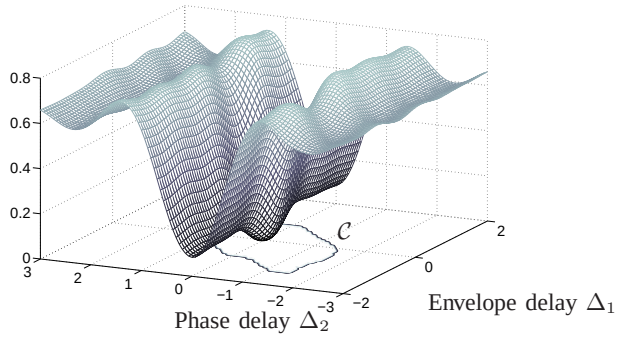

Fig. 3. Shape of criterion for a 16QAM, with the indication of the basin of attraction, such that the minimum can be obtained using a descent algorithm from any initial point in the basin.

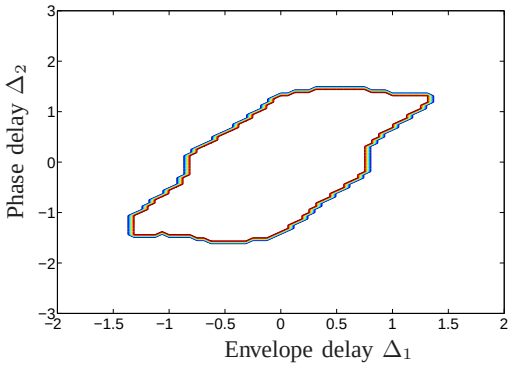

Fig. 4. Domain of convergence $\mathcal{C}$ for a 16QAM with a Nyquist square root shaping filter with roll-off of 0.22, which corresponds to the 3GPP standard. Larger domains are obtained when the roll-off increases (smoother error function).

III. A CORRECTION ALGORITHM

A. Principle and derivation of the correction algorithm

The basic idea is to introduce two advances, say μ_1 and μ_2, as indicated in Fig. 5 in the envelope and phase paths. Then the advances are tuned so as to minimize some distance, e.g. the quadratic distance, between the resulting observation and the original aligned signal: the optimum values of the two advances will exactly compensate the delays introduced by the analog paths.

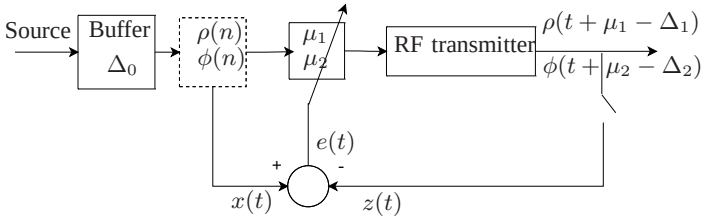

Fig. 5. Principle of the feedback loop for delays correction: two advances μ_1 and μ_2 are introduced in the main path (the original signal is buffered so as to be able to compute these advances). The remaining delays at output are $\Delta_1 - \mu_1$ and $\Delta_2 - \mu_2$. The output is compared to the original aligned input, and μ_1, μ_2 are adjusted so as to minimize this error. The two signals are synchronized when $\mu_1 = \Delta_1$ and $\mu_2 = \Delta_2$.

With the advances μ_1 and μ_2 introduced in the envelope and

phase paths, the output becomes

$$z(t) = \rho(t+\mu_1-\Delta_1)\cos(\phi(t+\mu_2-\Delta_2)). \quad (8)$$

The related mean square error is

$$\begin{aligned} J(\mu_1,\mu_2) &= \mathrm{E}\big[|e(t)|^2\big] = \mathrm{E}\big[|x(t)-\rho(t_1)\cos(\phi(t_2))|^2\big], \\ &= 4R(0,0) - 4R(\Delta_1-\mu_1,\Delta_2-\mu_2). \end{aligned} \quad (9)$$

where we noted $t = nT$, with T the sampling period, and also used $t_1 = t+\mu_1-\Delta_1$ and $t_2 = t+\mu_2-\Delta_2$ in order to simplify the expressions.

As above-mentioned we do not have a closed-form for this criterion nor, of course, a direct explicit solution for its minimizers. But as we have noticed from the general shape of the criterion, we can reach the solution with a descent algorithm. We can use a gradient algorithm that consists in iterating

$$\begin{aligned} \mu_1(k+1) &= \mu_1(k) - \gamma_1(k)\left.\frac{\partial J}{\partial \mu_1}\right|_{\mu_1=\mu_1(k)} \\ \mu_2(k+1) &= \mu_2(k) - \gamma_2(k)\left.\frac{\partial J}{\partial \mu_2}\right|_{\mu_2=\mu_2(k)} \end{aligned} \quad (10)$$

where γ_1 and γ_2 are adaptation steps. The gradients are computed according to

$$\frac{\partial J(\mu_1,\mu_2)}{\partial \bullet} = \frac{\partial \mathrm{E}\left[|e(t)|^2\right]}{\partial \bullet} = 2\mathrm{E}\left[\frac{\partial e(t)}{\partial \bullet} e(t)\right], \quad (11)$$

In practice, we have to resort to an approximation of the theoretical algorithm, using an appropriate approximation of the unknown theoretical expectations. A classical solution is to adopt a stochastic gradient algorithm which consists in using the instantaneous gradient rather than the statistical average, and in updating the equations at each new sample, at the rate T. This leads to the two updating rules for μ_1 and μ_2:

$$\begin{aligned} \mu_1(n+1) &= \mu_1(n) + \gamma_1(n)\left.\frac{d\rho(u)}{du}\right|_{t_1}\cos\phi(t_2)\, e(t) \\ \mu_2(n+1) &= \mu_2(n) + \gamma_2(n)\rho(t_1)\left.\frac{d\cos\phi(u)}{du}\right|_{t_2} e(t) \end{aligned} \quad (12)$$

In this approach, we have to adjust the two advances μ_1 and μ_2 and apply them to the input signal. Of course, working with digital signals implies that the data are only available at sampling points. Adopting very high sampling frequencies in order to get some required precision, is not an efficient solution with respect to cost, power consumption, and realization. A classical solution for tuning delays/advances from available data samples is digital interpolation. In order to be able to compute the advances by digital interpolation, we need will to dispose of some samples in the future of the current point. Therefore the procedure include a buffering of a few samples and the introduction of a small delay, say Δ_0, with respect to the message delivered to the transmitter. Let us now turn to the description of the interpolation procedure.

The task of approximating a function given a series of samples is solved, in numerical analysis, by Lagrange interpolation. A benefit of polynomial interpolators is that they can be implemented very efficiently in hardware, and that coefficients can be computed in real time. An efficient structure was devised by Farrow [25]. A recent improvement is given in [26]. Furthermore, in such structures, the delay is directly adjustable without modification so that it is very suitable in adaptive synchronization problems. It is worth mentioning that in the last decade, many solutions have been proposed for the synthesis and optimization of adjustable fractional delay filters, especially suitable in the case of large bands or when strong anti-aliasing is needed. In our context, the over sampling ratio is high and the frequency response of the interpolators is very flat in magnitude and linear in phase in the region of interest. Therefore, we simply adopt here a standard Lagrange interpolator, implemented using a Farrow structure. Performances and comparisons with respect to the choice of interpolator and with respect to the order are given in [21]. We select here a 5^{th} order Lagrange interpolator as an interesting trade off between performances and complexity. For this interpolator, if x is a sampled sequence at the rate T, then the interpolated value $x(m,\tau)$ at the time $(m+\tau)T$ is computed by

$$\begin{aligned} x(m,\tau) &= \tfrac{(\tau^2-1)(\tau-2)\tau}{24}x(m-2) \\ &- \tfrac{(\tau^2-4)(\tau-1)\tau}{6}x(m-1) + \tfrac{(\tau^2-1)(\tau^2-4)}{4}x(m) \\ &- \tfrac{(\tau^2-4)(\tau+1)\tau}{6}x(m+1) + \tfrac{(\tau^2-1)(\tau+2)\tau}{24}x(m+2). \end{aligned} \quad (13)$$

The computational load of algorithm (12) is of about 6 real multiplications per iteration. We have to compute the error and two derivatives that can be simply approximated by finite differences. Of course, we also have the cost of interpolation in the two branches, which has a complexity of p^2 for the Farrow structure and of $3p-1$ for Candan structure, where p is the interpolation order.

An important point concern the gradient computation: the derivative is evaluated on the output signal, at current time for the two components. This imposes a quadrature demodulation in order to separate the envelope and phase of $Z(t)$.

Moreover, the algorithm structure includes tracking capabilities, that are important in case of a non stationnary environment. However its drawback, from the viewpoint of hardware realization and consumption, is that the feedback involves a quadrature demodulation of the output of the transmitter. The suboptimal version below eliminate this need and can function with a simple demodulation or down-conversion.

B. A suboptimal version

It is clear that when the correction algorithm approaches the optimum solution, that is when $\mu_i \to \Delta_i$, we have of course $t_i = t+\mu_i-\Delta_i \to t$, and

$$\left.\frac{d\rho(u)}{du}\right|_{t_1}\cos\phi(t_2 \approx \left.\frac{d\rho(u)}{du}\right|_{t}\cos\phi(t) \quad (14)$$

and

$$\rho(t_1)\left.\frac{d\cos\phi(u)}{du}\right|_{t_2} \approx \rho(t)\left.\frac{d\cos\phi(u)}{du}\right|_{t}. \quad (15)$$

This simply means that we may afford to substitute the computations at times t_i by the similar computations at time t. These computations can be done using the reference signal at current time, rather than requiring the quadrature demodulation

of the output. In such a case, the update equations for μ_1, μ_2 become

$$\begin{aligned} \mu_1(n+1) &= \mu_1(n) + \gamma_1(n)\, \frac{d\rho(u)}{du}\Big|_t \cos\phi(t)\, e(t), \\ \mu_2(n+1) &= \mu_2(n) + \gamma_2(n)\rho(t)\, \frac{d\cos\phi(u)}{du}\Big|_t e(t). \end{aligned} \tag{16}$$

With respect to the original correction algorithm, the updates only differ by the the factor in front of the error term $e(t)$. Therefore, the direction of descent is not affected if these factors have the same sign. Hence, in the domain where these factors have the same sign, the algorithms will converge to the same and true solution. This can give a very rough idea of the domain of convergence of the new algorithm. As we work with random processes, this condition shall be considered in mean. We thus consider the domains $\mathcal{S}_i$ of the differences $\mu_i - \Delta_i$ defined by

$$\mathcal{S}_1: \quad \mathrm{E}\left[\frac{d\rho(u)}{du}\Big|_{t_1} \cos\phi(t_2)\, \frac{d\rho(u)}{du}\Big|_t \cos\phi(t) \right] \geq 0 \tag{17}$$

$$\mathcal{S}_2: \quad \mathrm{E}\left[\rho(t_1)\, \frac{d\cos\phi(u)}{du}\Big|_{t_2} \rho(t)\, \frac{d\cos\phi(u)}{du}\Big|_t \right] \geq 0 \tag{18}$$

where the factors exhibit the same sign in statistical mean. Now, as an heuristic guideline, we consider the domain $\mathcal{C}' = \mathcal{C} \cap \mathcal{S}_1 \cap \mathcal{S}_2$, the intersection of the original convergence domains with the $\mathcal{S}_i$. This domain is given in Fig. 6. Compared to Fig. 3, we observe that the domain have been reduced by the approximation. However, the previous condition only gives the region where the two algorithms almost follow the same trajectories. The suboptimal algorithm still converges for delays outside of these regions, but along different paths. The exact determination of the convergence domain of the two coupled non linear equations (16) is a formidable, if not impossible task.

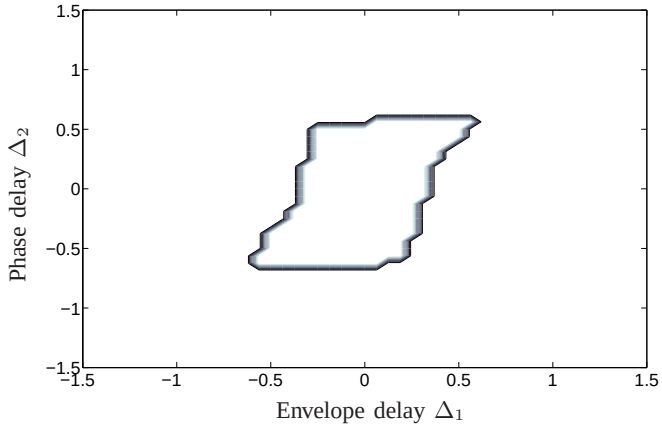

Fig. 6. Domains $\mathcal{C}' = \mathcal{C} \cap \mathcal{S}_1 \cap \mathcal{S}_2$ as the intersection of the domain of convergence $\mathcal{C}$ and the domains $\mathcal{S}_i$ where the gradients evaluated at the system input, at time t, or at its output affected by a delay $\delta_i = \Delta_i - \mu_i$ have the same sign in mean. This gives the indication of the domain where the suboptimal algorithm has the same behavior as the original one.

C. Results and comparisons

Performances have been evaluated using the simulation model presented section II-A and figure Fig. 2. The two algorithms (12) and (16), as well as the interpolator (13) were implemented. under ADS. Figure 7 presents the results obtained with the optimum correction algorithm in the case $\Delta_1 = 0.95\ T_s$ and $\Delta_2 = 0.45\ T_s$, for 20 different realizations of a 16QAM sequence. We can observe that the algorithm converge to the correct solutions.

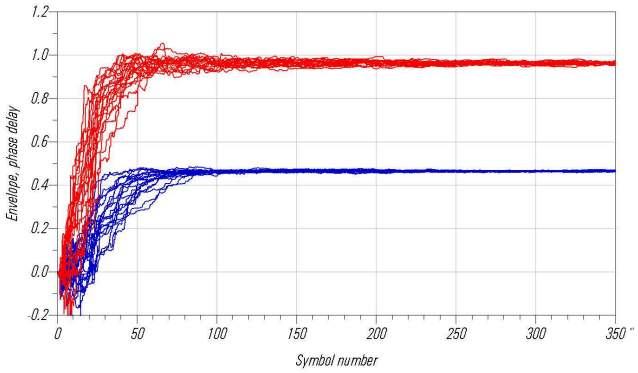

Fig. 7. Results for the optimum correction algorithms in the case $\Delta_1 = 0.95$ and $\Delta_2 = 0.45$, for 20 different realizations of a 16QAM sequence.

Table II reports the main figures for the algorithms for different test cases. Both algorithms have the same performances after the initial convergence. They exhibit a very large improvement for the EVM (falling from 38% in worst case to about 0.4%), as well as for the spectral regrowths, which are reduced to less than 58 dBc. The standard deviation for the estimates of the delays is less than 0.5% of the symbol period. Defining the mean convergence time T_c as the delay to reach the final value with a precision of 0.5% of T_s, we obtain that the suboptimal algorithm converges a bit slower than the original one. Convergence speed, bias and variance are also linked to the choice of the adaptation steps γ_1 and γ_2. All the examples in Table II used the same values (normalized values to the signal power) $\gamma_1 = \gamma_2 = 0.5$. The fact that the choice is not really crucial since there exists a large range of reasonable values for the adaptation steps, with respect to bias, variance and EVM is discussed in [21]. These results underline the fact that the synchronisation has to be processed in an initial calibration step.

Finally, we illustrate the tracking capabilities of the procedure in case of variations of the delays during time. For instance, a drift of some element in the system can induce a slow variation while a commutation between functional modes of the transmitter causes a sudden rupture. The simulation results presented in Fig. 8 shows that the solution is of interest in such situations. It enables to track drifts and plays the role of an autocalibration procedure in case of ruptures. Note that in tracking mode, the algorithm can be updated at a different (much slower) rate than the original sampling rate. It can also be activated only in the case of detection of a sufficient drift from the nominal performances, or synchronously to a commutation of mode in the system.

Δ_1	Δ_2	Tc		**EVM** (%)		**Relative Spectrum @**$3.5\ MHz$	
		Opt	Sub Opt	Initial	After	Initial	After
$0.2T_s$	$1.1T_s$	$150T_s$	$190T_s$	38%	0.4%	-30 dBc	-58 dBc
$0.45T_s$	$0.95T_s$	$140T_s$	$160T_s$	25%	0.4%	-32 dBc	-59 dBc
$0.5T_s$	$0.12T_s$	$130T_s$	$150T_s$	20%	0.4%	-35 dBc	-60 dBc
$0.1T_s$	$0.2T_s$	$85T_s$	$110T_s$	5.5%	0.4%	-48 dBc	-68 dBc

TABLE II
ALGORITHMS PERFORMANCES

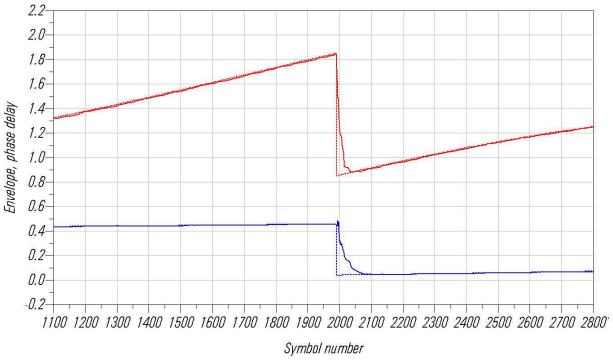

Fig. 8. Illustration of the behavior of the optimum algorithm in case of nonstationarities. This shows that the algorithm can account for slow drifts of the analog system (tracking capabilities) as well as sudden ruptures that may occur in multimodes solutions (autocalibration capabilities).

IV. GAIN AND PHASE IDENTIFICATION

The results presented above were obtained without considering the gain and phase offset introduced by the transmitter. Indeed, even with the knowledge of the output power and the global phase shift introduced by the transmitter, it often remains an uncertainty about the gain (0.5 dB for example) and the phase shift of the signal. We first examine the consequences of these uncertainties on the behavior of the algorithms. We show that the algorithms are robust to these errors but that the variance of estimates increases. We then show that it is possible to tackle this problem by the introduction of an identification step of both the gain and phase offset.

A. Consequences of uncertainty on gain and phase offset

The direct consequence is that the mean square error between the input and output of the system is not null anymore when they are perfectly aligned: if $Z(t)$, the standard output

$$Z(t) = \rho(t-\Delta_1)e^{j\phi(t-\Delta_2)},$$

is affected by a complex gain $K = |K|e^{j\theta}$ the error between the complex envelopes becomes

$$\bar{J}(\Delta_1,\Delta_2) = \mathrm{E}\left[|X(t)-Z(t)|^2\right] = (1+|K|^2)\mathrm{E}\left[\rho(t)^2\right] - 2|K|\mathrm{E}\left[\rho(t)\rho(t-\Delta_1)\cos(\phi(t)-\phi(t-\Delta_2)-\theta)\right], \quad (19)$$

and we obtain $J(0,0) = (1+|K|^2-2|K|\cos(\theta))\mathrm{E}\left[\rho(t)^2\right]$. Hence, even when the signals are aligned, the error is not null. Furthermore, we need to check if this value remains a minimum of the criterion. Let us now check that the criterion is still minimum in the aligned case. We note $\epsilon(t) = \phi(t)-\phi(t-\Delta_2)$ the difference process. Its probability density function is known and can be found in [24, 8.82, p. 369] for instance. The phase $\phi(t)$ of a Gaussian process being uniformly distributed on $[0,2\pi]$, we readily obtain that $\mathrm{E}[\epsilon(t)] = 0$. As far as the variance is concerned, it is simply given by

$$\mathrm{E}\left[\epsilon(t)^2\right] = 2R_\phi(0) - 2R_\phi(\Delta_2) \quad (20)$$

with $R_\phi(\Delta_2)$ the autocorrelation function of the phase, which can be expressed as a serie [24, 8.81, p. 369]
If we approximate $\epsilon(t)$ and $\rho(t)\rho(t-\Delta_1)$ as uncorrelated variables, an approximation that is reasonable for small delays ($\rho(t)$ and $\phi(t)$ are independent), we have

$$\bar{J}(\Delta_1,\Delta_2) \approx (1+|K|^2)R_\rho(0) - 2|K|R_\rho(\Delta_1)\left(\mathrm{E}\left[\cos(\epsilon)\right]\cos(\theta) + \mathrm{E}\left[\sin(\epsilon)\right]\sin(\theta)\right) \quad (21)$$

with $R_\rho(\tau)$ the autocorrelation function of the envelope $\rho(t)$. Since $\epsilon(t)$ is small, we can expand the expression in ϵ, keep the terms of the development up to the second order and take the expectation using (20). This leads to

$$\bar{J}(\Delta_1,\Delta_2) = (1+|K|^2)R_\rho(0) - 2|K|R_\rho(\Delta_1)\left(1-R_\phi(0)+R_\phi(\Delta_2)\right)\cos(\theta). \quad (22)$$

Consider now Δ_2 fixed and small enough so that $R_\phi(0) - R_\phi(\Delta_2) < 1$. Then, since $R_\rho(\tau)$ is maximum for $\tau = 0$, the criterion is minimum for $\Delta_1 = 0$, provided that $\cos\theta$ is positive. If now Δ_1 is fixed, since $R_\rho(\tau)$ is always positive and $1-(R_\phi(0)-R_\phi(\tau))$ is maximum for $\tau = 0$, we obtain that the criterion is minimum for $\Delta_2 = 0$ if $\cos\theta$ is positive. Therefore, we finally have, as expected, that $J(0,0)$ is a minimum with respect to the two delays. The condition $\cos\theta > 0$ is important and means that the algorithms cannot cope with unknown phase offsets greater than $\pi/2$ (but of course such critical value cannot occur in a correct design). The deformation of the criterion with a phase shift is illustrated in Fig. 9, where we report the criterion with respect to Δ_2, with $\Delta_1 = 0$ fixed, for several values of the phase shift θ. When the phase shift becomes greater than $\pi/2$, then the minimum becomes a maximum.
These results show that the algorithms are robust and can be used even with an imperfect knowledge of the gain, which is important in practical situations. But since this error, whose power converges to a finite value, is used directly in the updates equations of the stochastic algorithms, the convergence is affected by fluctuations. This is illustrated in Fig. 10 where we present a typical result of the optimum algorithm with 0.5 dB of gain mismatch and 10° of phase offset.

B. Identification of gain and phase unknowns

Although the algorithms converge in mean to the correct solution, the mean square error is not zero at the optimum and the solution is corrupted by a residual noise. Therefore, it

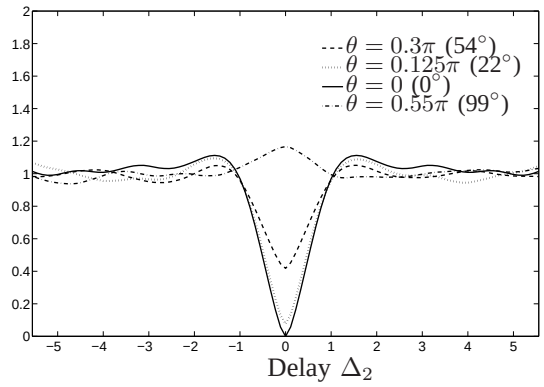

Fig. 9. Criterion with phase mismatches θ. The minimum, whose value increases, remains at $\Delta_2 = 0$, for all phase offsets lower than $\pi/2$.

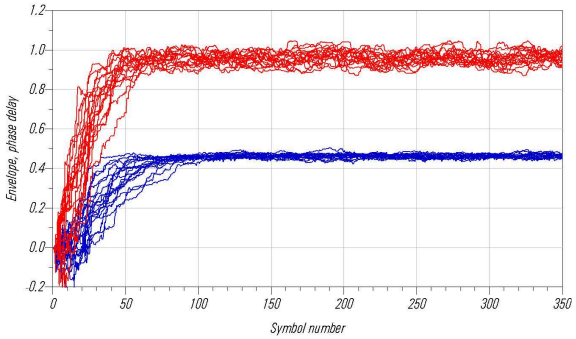

Fig. 10. Delay identification with 0.5 dB of gain mismatch and 10°of phase offset in the case $\Delta_1 = 0.95$ and $\Delta_2 = 0.45$: the algorithm still converges but is corrupted by noise. The fluctuations imply spectral regrowths that can prevent the respect of requirements in performances.

is useful to look for a solution that reduces this residual noise, since it degrades both EVM and spectral performances. Along the lines of the previous developments, the natural solution is to try to identify or correct the unknown gain. In the present case, it is not useful to correct the gain in the transmitter path since after all the receiver has its own equipment for synchronization and gain control, and since other phase shifts and attenuation occur during transmission. Therefore, the gain can be accounted for in the feedback loop, and we can adopt an identification type structure. The complete structure for delays correction together with the account for uncertainty in gain and phase shift is given in Fig. 11.

As previously, we derived two algorithms for the optimum and suboptimal algorithms. For the optimum case, the algorithm takes into account the in phase and quadrature signals, whereas for the suboptimal delays correction algorithm, this solution only requires the in-phase component of the output. Indeed, the computations on the envelope and phase are done on the digital signals already available at the input. Using the same principle for both versions of the algorithm, we will demonstrate the formulation of the sub optimum version here. With the notations in Fig. 11, the error is given by

$$e(t) = G\rho(t)\cos(\phi(t)+\psi) - K\rho(t-\Delta_1)\cos(\phi(t-\Delta_2)+\theta). \quad (23)$$

and we look for G and ψ that minimize the mean square

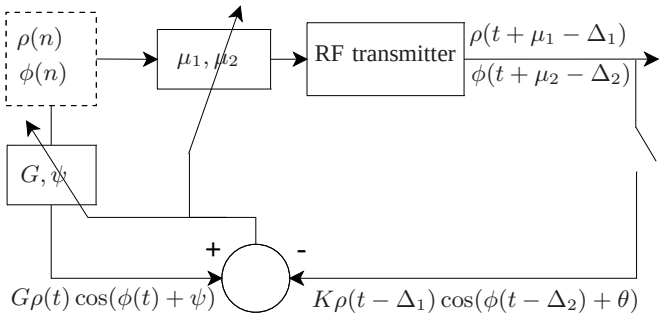

Fig. 11. Complete structure for delays correction with identification of possible gain and phase shift. The same error $e(t)$ is used to correct the delays Δ_1 and Δ_2 introduced in the transmitter and to identify gain variation and phase shift.

error $J(G,\psi) = \mathrm{E}\left[|e(t)|^2\right]$. As before, we derive a gradient solution and implement a stochastic gradient algorithm:

$$\begin{aligned} G(n+1) &= G(n) - \gamma_3(n)\rho(t)\cos(\phi(t)+\psi(n))e(t) \\ \psi(n+1) &= \psi(n) - \gamma_4(n)G(n)\rho(t)\sin(\phi(t)+\psi(n))e(t). \end{aligned} \quad (24)$$

In terms of the complex gain $\tilde{G} = G\exp(j\psi) = G_r + jG_i$ and the complex envelopes, the error can also be expressed as $e(t) = \mathrm{Re}\left(\tilde{G}X(t) - Z(t)\right)$, which leads to the recursions

$$\left\{ \begin{array}{rcl} G_r(n+1) &=& G_r(n) - \gamma_3(n)\rho(t)\cos(\phi(t))e(t) \\ G_i(n+1) &=& G_i(n) + \gamma_4(n)\rho(t)\sin(\phi(t))e(t) \end{array} \right. \quad (25)$$

This formulation is much more interesting for the implementation, since it only involves available signals and does not require evaluations of trigonometric functions of the estimates, as in (24). For completeness, let us also note that the algorithm derived from the complex error $e(t) = \tilde{G}X(t) - Z(t)$, which requires a quadrature demodulation of the output, is

$$\tilde{G}(n+1) = \tilde{G}(n) - \gamma_3 X^*(t)\left(\tilde{G}(n)X(t) - Z(t)\right). \quad (26)$$

C. Results

In the very same conditions as in Fig. 10, that is with 0.5 dB of gain variation and a phase offset of 10°, with $\Delta_1 = 0.95$ and $\Delta_2 = 0.45$, the introduction of the correction of gain and phase in the feedback loop using (25) leads to results very similar to the original results in Fig. 7 without gain and phase perturbations. These results are quantified in Table III where we consider different scenarios for the gain and phase mismatches. We obtain a large improvement both for the EVM (that falls to about 0.5% near the result without gain and phase mismatch) and for the spectrum at 3.5 MHz, which is attenuated to less than 58 dBc. The only concern is a slower mean convergence which is the price to pay to account for these further mismatches.

V. Conclusions

Polar based transmitter architectures, which are already recognized solutions, are regarded as very promising structures for future realizations. In this work, we considered the critical issue of delays mismatches in polar based transmiter architectures, which degrades the performances, particularly with

Gain mismatch	phase mismatch	Tc		**EVM (%)**		**Relative Spectrum @**$3.5\ MHz$	
		Opt	Sub Opt	without identification	with identification	without identification	with identification
3 dB	45°	350 T_s	420 T_s	23%	0.5%	-40 dBc	-58 dBc
1 dB	30°	300 T_s	400 T_s	11%	0.5%	-47 dBc	-58 dBc
0.5 dB	10°	280 T_s	350 T_s	3.4%	0.5%	-55 dBc	-59 dBc
0.2 dB	2°	250 T_s	320 T_s	0.8%	0.5%	-58 dBc	-60 dBc

TABLE III
ALGORITHMS PERFORMANCES WITH GAIN IDENTIFICATION FOR $\Delta_1 = 0.45\ T_s$ AND $\Delta_2 = 0.95\ T_s$

increasing data rates. We address this problem by digital signal processing. Based on the minimization of the mean square error, we present a baseband algorithm for the correction of delays mismatches. We also propose a suboptimal version that minimizes the realization and implementation costs. We address the fact that the system can also introduce a gain and phase shift. Although it is not necessary to compensate these further mismatches from the system viewpoint, it is useful to account for them in the feedback loop to preserve good performances. This is achieved by the insertion of an identification procedure. Simulation results show a high improvement in the performances, with an EVM below 0.5% and a spectrum level at 3.5 MHz lower than -58 dBc in 30 kHz bandwidth. This demonstrates the real interest of these approaches for the design and optimization of current and future transceivers.

The exact strategy for the compensation of the delays in a polar architecture has probably to be defined on a case-by-case basis. Since there is no possible useful data transmission during the convergence time, a initial calibration may employ the first correction algorithm, while the suboptimal version can be reserved for refinement and tracking of nonstationarities during operational modes. Of course, the feedback loop can also be used for other compensations, for instance ripples in the frequency response, and the correction algorithm shall cooperate with the compensation of nonlinearities of the power amplifier.

Although it is still possible to further optimize the elements of the transmitter in order to minimize the analog mismatches distorsions, we believe that it is also possible to relax some of the constraints and report a part of the analog complexity to the baseband digital signal processing.

ACKNOWLEDGMENT

The authors are indebted to early readers of this manuscript. The authors also acknowledge O. Venard for several discussions and improvements of the paper.

REFERENCES

[1] F. Raab, P. Asbeck, S. Cripps, P. Kenington, Z. Popovic, N. Pothecary, J. Sevic, and N. Sokal, "Power amplifiers and transmitters for RF and microwave," *IEEE Transactions on Microwave Theory and Techniques*, vol. 50, pp. 814–826, 2002.

[2] A. Hietala, "A quad-band 8PSK/GMSK polar transceiver," *IEEE Journal of Solid-State Circuits*, vol. 41, pp. 1133–1141, 2006.

[3] J. Groe, "Polar transmitters for wireless communications," *IEEE Communications Magazine*, vol. 45, pp. 58–63, 2007.

[4] J. Groe, "A multimode cellular radio," *IEEE Transactions on Circuits and Systems II: Express Briefs*, vol. 55, pp. 269–273, 2008.

[5] L. Kahn, "Single-sideband transmission by envelope elimination and restoration," *Proceedings of the IRE*, vol. 40, no. 7, pp. 803–806, July 1952.

[6] R. Staszewski, J. Wallberg, S. Rezeq, C.-M. Hung, O. Eliezer, S. Vemulapalli, C. Fernando, K. Maggio, R. Staszewski, N. Barton, M.-C. Lee, P. Cruise, M. Entezari, K. Muhammad, and D. Leipold, "All-digital PLL and transmitter for mobile phones," *IEEE Journal of Solid-State Circuits*, vol. 40, no. 12, pp. 2469–2482, Dec. 2005.

[7] D. Rudolph, "Out-of-band emissions of digital transmissions using Kahn EER technique," *IEEE Transactions on Microwave Theory and Techniques*, vol. 50, pp. 1979–1983, 2002.

[8] G. Strasser, B. Lindner, L. Maurer, G. Hueber, and A. Springer, "On the spectral regrowth in polar transmitters," in *Microwave Symposium Digest, 2006. IEEE MTT-S International*, 2006, pp. 781–784.

[9] J.-F. Bercher, A. Diet, C. Berland, G. Baudoin, and M. Villegas, "Monte-carlo estimation of time mismatch effect in an OFDM EER architecture," in *Proceedings of the 2004 IEEE Radio and Wireless Conference*, 19-22 Sept. 2004, pp. 283–286.

[10] M. Markovic and H. Modi, "Feasibility of EER transmitters for 3GPP applications," in *IEEE Annual Wireless and Microwave Technology Conference, WAMICON '06*, 2006, pp. 1–2.

[11] W.-F. Loke, M.-W. Chia, and P.-Y. Chee, "Design considerations for multi-band OFDM polar transmitter of UWB system," *Electronics Letters*, vol. 43, 2007.

[12] B. Priyanto, T. Sorensen, O. Jensen, T. Larsen, T. Kolding, and P. Mogensen, "Impact of polar transmitter imperfections on UTRA LTE uplink performance," in *Norchip, 2007*, 2007, pp. 1–4.

[13] W. B. Sander, S. V. Schell, and B. L. Sander, "Polar modulator for multimode cell phones," *Proceedings of the IEEE 2003 Custom Integrated Circuits Conference*, pp. 439–445, 2003.

[14] K. Waheed, R. B. Staszewski, and S. Rezeq, "Curse of digital polar transmission: Precise delay alignment in amplitude and phase modulation paths," in *IEEE International Symposium on Circuits and Systems, ISCAS 2008*, 2008, pp. 3142–3145.

[15] P. Morgan, "Highly integrated transceiver enables high-volume production of GSM/EDGE handsets," *RFdesign*, pp. 36–42, Jul. 2006.

[16] J.-K. Jau and T.-S. Horng, "Linear interpolation scheme for compensation of path delay difference in an envelope elimination and restoration transmitter," in *Proceedings of Asia-Pacific Microwave Conference, 2001. APMC 2001*, vol. 3, 2001, pp. 1072–1075 vol.3.

[17] J. Mártires, C. Borg, and T. Larsen, "Differential delay equalization in a Kahn EER transmitter," in *ST Mobile & Wireless Communications Summit, nr. 15th*, Myconos, Grækenland, Jun. 2006.

[18] C. Zhi and H. Yang, "A new adaptive delay method for wideband Kahn's RF power amplifiers," in *IEEE Tenth International Symposium on Consumer Electronics*, 2006, pp. 1–4.

[19] F. Wang, A. Yang, D. Kimball, L. Larson, and P. Asbeck, "Design of wide-bandwidth envelope-tracking power amplifiers for OFDM applications," *IEEE Transactions on Microwave Theory and Techniques*, vol. 53, pp. 1244–1255, 2005.

[20] J.-F. Bercher and C. Berland, "Adaptive time mismatches identification and correction in polar transmitter architecture," in *2007 European Conference on Wireless Technologies*, 2007, pp. 78–81.

[21] J.-F. Bercher and C. Berland, "Envelope and phase delays correction in an EER radio architecture," *Analog Integrated Circuits and Signal Processing*, vol. 55, pp. 21–35, Apr. 2008.

[22] "3GPP TS 125 213, version 7.0.0, release 7 and 3GPP TS 125 101, version 7.6.0, release 7."

[23] S. C. Cripps, *Advanced Techniques in RF Power Amplifier Design*. Artech House, May 2002.

[24] B. R. Levin, *Fondements théoriques de la radiotechnique statistique*. Moscow: Éditions Mir, 1979, vol. 1.

[25] C. W. Farrow, "A continuous variable digital delay element," in *Proc. IEEE Int. Symp. Circuits Systems*, 1988, pp. 2641–2645.

[26] C. Candan, "An efficient filtering structure for lagrange interpolation," *IEEE Signal Processing Letters*, vol. 14, no. 1, pp. 17–19, Jan 2007.